View metadata, citation and similar papers at core.ac.uk

brought to you by CORE

provided by Warwick Research Archives Portal Repository

THE UNIVERSITY OF
WARWICK

Original citation:
George, I, Becagli, F., Liu, H. Y., Wu, J., Tanga, M. and Beanland, R.. (2015) Dislocation filters in GaAs on Si. Semiconductor Science and Technology, 30 (11). 114004. http://dx.doi.org/10.1088/0268-1242/30/11/114004
Permanent WRAP url:
http://wrap.warwick.ac.uk/75677

Copyright and reuse:
The Warwick Research Archive Portal (WRAP) makes this work of researchers of the University of Warwick available open access under the following conditions.

This article is made available under the Creative Commons Attribution- 3.0 Unported (CC BY 3.0) license and may be reused according to the conditions of the license. For more details see http://creativecommons.org/licenses/by/3.0/
A note on versions:
The version presented in WRAP is the published version, or, version of record, and may be cited as it appears here.

For more information, please contact the WRAP Team at: publications@warwick.ac.uk

http://wrap.warwick.ac.uk/

IOPscience iopscience.iop.org

Home Search Collections Journals About Contact us My IOPscience

Dislocation filters in GaAs on Si

This content has been downloaded from IOPscience. Please scroll down to see the full text.

2015 Semicond. Sci. Technol. 30 114004

(http://iopscience.iop.org/0268-1242/30/11/114004)

View the table of contents for this issue, or go to the journal homepage for more

Download details:

IP Address: 137.205.202.97
This content was downloaded on 14/01/2016 at 09:45

Please note that terms and conditions apply.

OPEN ACCESS
IOP Publishing

Semiconductor Science and Technology

Semicond. Sci. Technol. **30** (2015) 114004 (5pp)

doi:10.1088/0268-1242/30/11/114004

Dislocation filters in GaAs on Si

I George[1], F Becagli[1], H Y Liu[2], J Wu[2], M Tang[2] and R Beanland[1,3]

[1] Department of Physics, University of Warwick, Coventry CV4 7AL, UK
[2] Department of Electronic and Electrical Engineering, University College London, Torrington Place, London WC1E 7JE, UK

E-mail: r.beanland@warwick.ac.uk

Received 28 March 2015, revised 21 July 2015
Accepted for publication 22 July 2015
Published 15 October 2015

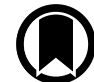

Abstract

Cross section transmission electron microscopy has been used to analyse dislocation filter layers (DFLs) in five similar structures of GaAs on Si that had different amounts of strain in the DFLs or different annealing regimes. By counting threading dislocation (TD) numbers through the structure we are able to measure relative changes, even though the absolute density is not known. The DFLs remove more than 90% of TDs in all samples. We find that the TD density in material without DFLs decays as the inverse of the square root of the layer thickness, and that DFLs at the top of the structure are considerably more efficient than those at the bottom. This indicates that the interaction radius, the distance that TDs must approach to meet and annihilate, is dependent upon the TD density.

Keywords: GaAs on Si, threading dislocations, dislocation filters

(Some figures may appear in colour only in the online journal)

1. Introduction

The inability to control threading dislocation (TD) density in heteroepitaxial layers has held back the deployment of many materials systems for some time. Perhaps the most widely studied system is GaAs on Si [1], which was the subject of intense work in the 1980s [2] but failed to become commercially viable. There are two main problems in this materials system; thermal expansion mismatch [3], and high TD density ρ_{TD}. Since GaAs has a higher thermal expansion coefficient (5.73×10^{-6} K^{-1}) than Si (2.6×10^{-6} K^{-1}), if a thick epitaxial GaAs layer is fully relaxed during growth at a high temperature it cracks during cooling [1, 4]. The solution is to use a thin epitaxial layer, since there is a critical thickness for cracking of epitaxial layers [5]. The origin of high TD densities is not fully understood—there is currently no model that can predict the TD density in any materials system—but it is known to be correlated with the three dimensional islands that form in the very first stages of growth [6]. It is also known that the TD density decreases with increasing layer thickness [3, 4, 7], but unfortunately the amount of material required to obtain a technologically viable TD density $\rho_{TD} < 10^5$ cm^{-2} is much larger than the critical thickness for cracking. There is no process window.

Apart from simply growing thick epitaxial layers [4, 7], it is possible to reduce TD densities more efficiently by design. In particular, thin strained layers have been used to encourage TDs to move, interact and annihilate for some time [8, 9], and have become known as dislocation filter layers (DFLs). However, there are few, if any, studies looking at the effect of DFLs in detail, and this is the motivation for the work described here. It is hoped that understanding of DFLs may allow them to be optimized sufficiently to allow the production of GaAs layers on Si that are both below the critical thickness for cracking and with low TD density.

2. Experiment

A typical DFL sample structure is shown in the cross section transmission electron microscopy (TEM) images of figure 1. Growth was performed on n-doped Si (001) substrates offcut by 4° towards [110] using solid-source molecular beam

[3] Author to whom any correspondence should be addressed.

Content from this work may be used under the terms of the Creative Commons Attribution 3.0 licence. Any further distribution of this work must maintain attribution to the author(s) and the title of the work, journal citation and DOI.

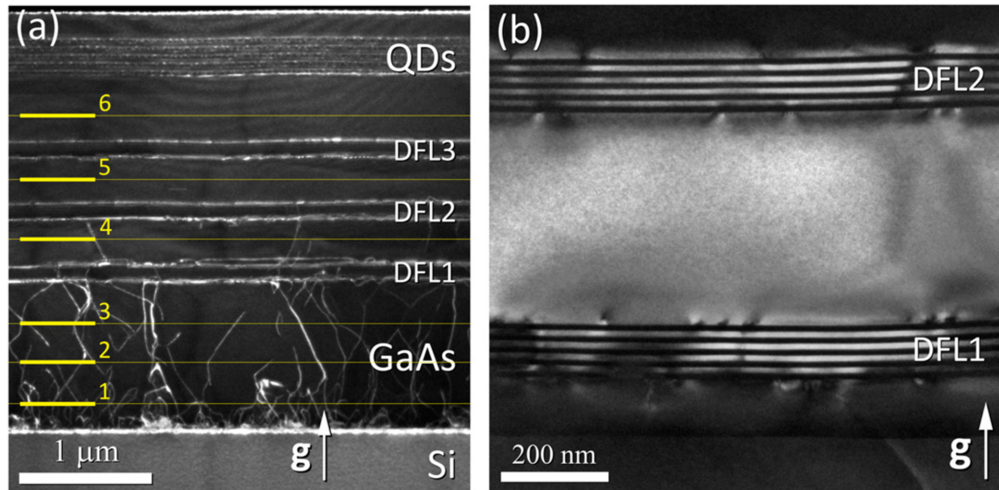

Figure 1. (a) A dark field weak beam, **g**, 2**g** 004 TEM cross section image of a typical epitaxial layer structure of GaAs on Si with three DFLs. The active region contains quantum dots (QDs), at the top of the structure. Dislocations were counted crossing the lines marked 1–6. (b) Dark field **g** 002 image of DFL1 and DFL2, showing the five 10 nm $In_xGa_{1-x}As$ layers (dark) and four 10 nm GaAs spacers in each. Misfit dislocations are visible at the upper and lower interfaces.

Table 1. The five samples examined in this study.

Sample	DFL composition	Anneal type
UCL203 R22	$x = 0.18$	0
UCL203 R23	$x = 0.18$	1
UCL203 R24	$x = 0.18$	2
UCL203 R28	$x = 0.16$	2
UCL203 R29	$x = 0.20$	2

epitaxy. Oxide desorption of the Si substrates was performed at 900 °C for 10 min The substrates were then cooled down for the growth of a 30 nm GaAs nucleation layer at 370 °C followed by 170 nm of GaAs at 515 °C. An 800 nm buffer of GaAs was then grown at 660 °C, the first 100 nm of which was a 5:5 nm $Al_xGa_{1-x}As$:GaAs short-period superlattice. This was followed by three DFLs separated by 400 nm GaAs spacer layers. Each DFL consisted of five layers of 10 nm $In_xGa_{1-x}As$ separated by four 10 nm layers of GaAs. Following another 400 nm GaAs spacer layer an InAs/GaAs dot-in-a-well (DWELL) structure was grown at 510 °C, similar to that optimized on GaAs substrates.

Five samples were grown, listed in table 1. These samples, form two self-consistent experiments that examine the effects of (a) anneals during growth (samples R22, R23, R24) and (b) changing the composition of the DFLs (samples R24, R28, R29).

Sample R22 had no anneals (Anneal Type 0). Sample R23 experienced Anneal Type 1; following the 100 nm SPSL in the 660 °C GaAs buffer layer, growth was paused and the sample held under an As flux. The anneal consisted of a heating ramp to 750 °C (2 min), hold at 750 °C (6 min), and cooling ramp to 660 °C (2.5 min). Samples R24, R28 and R29 experienced Anneal Type 2, consisting of anneal Type 1 plus a similar procedure after each DFL, i.e. before each 400 nm GaAs spacer layer.

The efficacy of TD filters is often assessed using techniques such as defect etching, which provides a single measurement for each growth. In contrast, here we use TEM to examine the structure in detail, in particular the changes in dislocation density through the epitaxial layer. Cross section TEM specimens parallel to {110} were prepared using standard protocols, each of which typically yielded 30–60 μm of electron transparent area along the GaAs:Si interface. A series of images were taken using bright field **g** 220 diffraction conditions with the specimen tilted 5°–10° from the {110} zone axis, capturing the complete structure as shown in figure 2 while covering as wide a field of view as possible. The change in TD density ρ_{TD} through the epitaxial layer was measured by counting those which crossed six lines, as indicated in figure 1(a). Although it is not possible to give an absolute measure of ρ_{TD} without knowing the thickness of the TEM specimen, this technique allows relative measurements to be obtained that are statistically meaningful. In particular, by counting TDs below and above a DFL it is possible to measure the fraction removed. Importantly, the measurement relies on two assumptions. First, the thickness of the TEM specimen from bottom to top of the epitaxial structure must not change. The validity of this assumption was checked by examining the projected length of misfit dislocations in the GaAs:Si interface as well as the DFLs, and was found to be valid to better than 5% for all measurements. Second, not all TDs are visible in images obtained with a single **g**-vector and it is assumed that the behaviour of the invisible dislocations matches those of the visible ones. In a **g** 220 image, TDs with **b** = ½ [1–10] and ½[−110] give **g** · **b** = 0 and are invisible (two of the twelve possible Burgers vectors in a face centred cubic material). These are sessile TDs, unable to move by glide, similar to the **b** = ½[110] and ½[110] types (all other types being glissile on {111} planes). Numerical modelling of TDs ensembles [10] indicate an interchange between mobile and sessile TD populations, leading to a balance; thus between a sixth and a quarter of TDs are expected to be

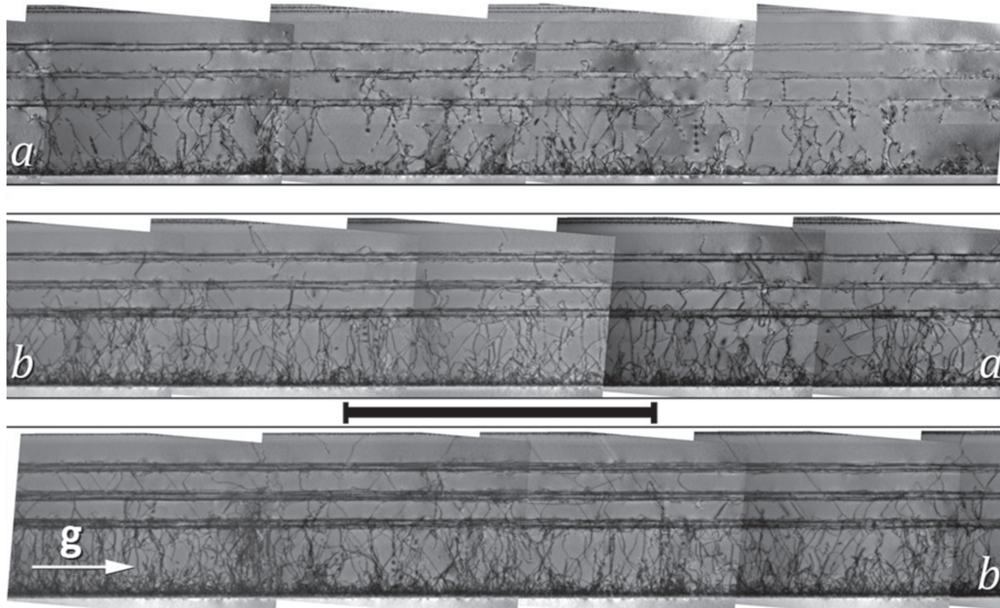

Figure 2. Montage of 13 bright field **g** 220 TEM cross section images (total width 48 μm) of UCL203 R22. The images join at edges *a*–*a* and *b*–*b*. The scale bar is 5 μm.

invisible in **g** 220 images. The aim was to count more than ten TDs at the uppermost line (typically giving counts up to a thousand at the lowest line). This was possible for all samples apart from R24, which had the lowest ρ_{TD} at the surface.

While it is not possible to give an accurate measurement of ρ_{TD}, we may obtain a rough estimate from images such as figure 2. The average TEM specimen thickness is of the order of 400 nm and there are 17 TDs that can be seen to reach the upper part of the structure over the ~50 μm width of the image. Taking into account the dislocations which are not visible in figure 2, this corresponds to a TD density of the order of one per square μm, i.e. $\rho_{TD} \sim 10^8\ \text{cm}^{-2}$.

In addition to the measurement of TD numbers through the structure, the density of misfit dislocations, ρ_{MD}, lying at the lower and upper interfaces of each DFL was obtained from bright field **g** 220 images at higher magnification. The misfit dislocation density was measured from the distance that contained a hundred misfit dislocations.

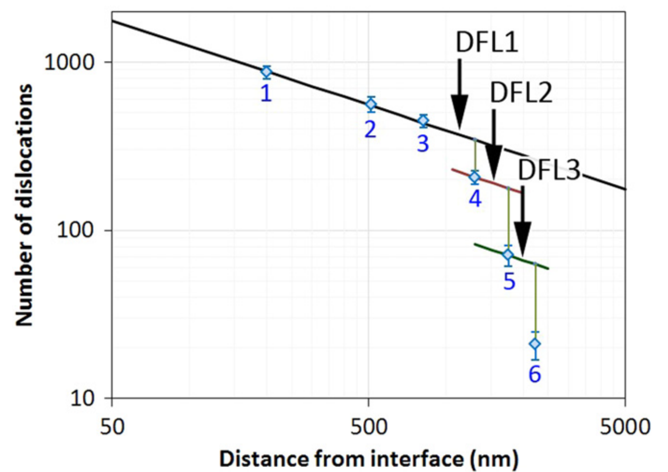

Figure 3. Log–log plot showing threading dislocation counts at the six positions in sample R23. A fit to the first three points is shown using a power law $\rho_{TD} = At^{-0.5}$. The effect of the DFLs is estimated by extrapolating this law to larger thicknesses.

3. Results

Counts of TDs at the first three lines, 300, 600 and 900 nm from The GaAs:Si interface, allows the 'natural' decrease in ρ_{TD} in thick layers to be measured. Previous measurements of the decrease in ρ_{TD} with thickness *h* have found a behaviour described by [11–13]

$$\rho_{TD} = Ah^m. \tag{1}$$

i.e. a power law, where *A* is a constant and the exponent *m* has a value of −1 [11], or −2 [12, 13]. We also find that a power law provides the best fit to our data (as opposed to, for example, a polynomial or exponential decay); however all of our data was consistent with $m = -½$, as can be seen in figure 3 for sample R23.

Since ρ_{TD} decreases with thickness even in the absence of a dislocation filter, the efficiency of a DFL can only be measured by taking this 'natural' decay into account. Thus, the curve fit to the first three points is extrapolated to higher thicknesses as shown in figure 3. We define the efficiency of a DFL to be the fraction of TDs it removes, i.e.

$$\text{Efficiency} = 1 - \frac{n(\text{meas})}{n(\text{predict})}, \tag{2}$$

where *n*(meas) is the number of dislocations counted at the line above the DFL, and *n*(predict) is the number of dislocations that would be present at that position by extrapolation of equation (1). The measured efficiency of the DFLs in all five samples is given in table 2. Errors in table 2 are based on the assumption that the spatial

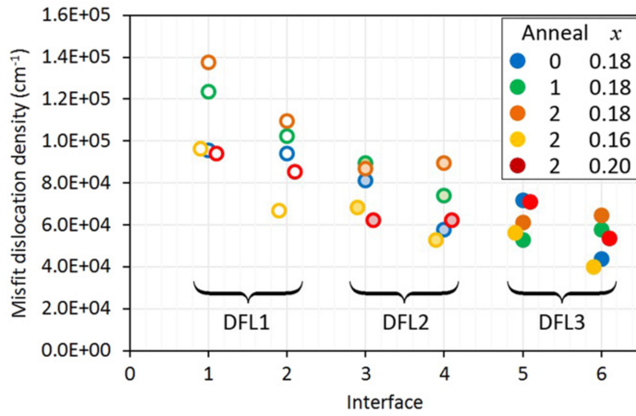

Figure 4. Misfit dislocation densities at the lower and upper interfaces of the DFLs.

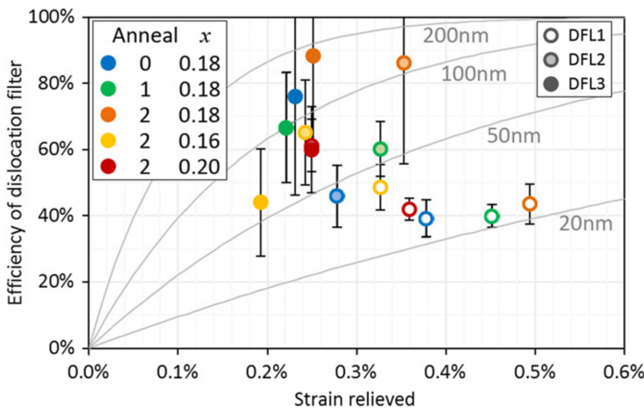

Figure 5. Plot of DFL efficiency versus the total strain relieved in the DFL interfaces. Curves are also shown for the predicted efficiency at different interaction radii $R = 20$, 50, 100, 200 nm.

Table 2. Efficiency of DFLs in the five samples.

Sample	DFL1	DFL2	DFL3	Total
UCL203 R22	(39 ± 6)%	(46 ± 9)%	(76 ± 30)%	92%
UCL203 R23	(40 ± 3)%	(60 ± 8)%	(67 ± 16)%	92%
UCL203 R24	(44 ± 6)%	(86 ± 30)%	(88 ± 30)%	99%
UCL203 R28	(49 ± 7)%	(65 ± 16)%	(44 ± 16)%	90%
UCL203 R29	(42 ± 3)%	(61 ± 8)%	(60 ± 13)%	91%

distribution of TDs follows a Poisson distribution, in which case the uncertainty in a count of n dislocations is $n^{0.5}$. The low numbers of dislocations that are counted for the upper DFLs produce large relative uncertainties.

The uncertainties are sufficient to mask any correlations due to different compositions (R24, 28, R29) or anneals (R22, R23, R24). Nevertheless, it is clear from table 2 that the upper DFLs tend to be more efficient than the lower ones.

Measurements of misfit dislocation density ρ_{MD} in the lower (L) and upper (U) interfaces of the DFLs are shown in figure 4. There is an obvious trend towards lower misfit dislocation densities in the upper DFLs, but once again any effects of composition or annealing cycle are masked by the spread in the data.

Figure 5 shows the efficiency of the DFLs as a function of the total strain relieved (i.e. proportional to the total misfit dislocation density in the DFL interfaces). This shows how the lower DFLs generally do not achieve high efficiencies for the removal of TDs, despite the higher density of misfit dislocations.

4. Discussion

The data clearly show several trends that do not agree with simple models of the behaviour of dislocations in strained layers and the effect of DFLs [9, 11, 13], indicating that there is still much to be learned about the behaviour of dislocations en masse. For example, in the material below the DFLs we find a decrease in TD density given by

$$\rho_{\mathrm{TD}} = Ah^{\frac{1}{2}}, \tag{3}$$

in contrast to previous work [12, 14], which found a decrease proportional to $1/h$ or $1/h^2$. The reasons for this are unclear at present, but may be related to the presence of the SPSL at the bottom of the structure, the overlying DFLs, or the different methodology used in this study.

Previous modelling [10] of interactions between mobile TDs in a strained epitaxial layer found that TD density decreases exponentially with the strain relaxed ε_r, i.e.

$$\rho_{\mathrm{TD}}(\varepsilon_r) = \rho_{\mathrm{TD}}^{(0)} \exp\left(\frac{-2Rq\varepsilon_r}{Db_{//}}\right), \tag{4}$$

where $\rho_{\mathrm{TD}}^{(0)}$ is the TD density immediately below the DFL, q is the fraction of encounters between TDs that lead to an annihilation ($q = ¼$ if there are equal numbers of all possible Burgers vectors), D is a geometrical factor ($D = ½$ in the case of a rectangular dislocation array), $b_{//}$ is the Burgers vector component parallel to the interface and R is the 'interaction radius'. Curves corresponding to equation (4) for several different values of R are shown in figure 5; it is clear that none of these curves describe the observed behaviour.

Despite the failure of the model, there can be no doubt that the basic tenet—i.e. that movement of TDs leads to reactions and annihilations—still holds. It is therefore worth examining the assumptions of the model used to obtain equation (4). In particular, the four parameters R, q, D and $b_{//}$ were all assumed to be constant and independent of other parameters. The results shown in figure 5 suggest that the interaction radius is not just sensitive to the strain state, as found by Fertig *et al* [15] but is also determined by the TD density ρ_{TD}. Furthermore, the volume of material sampled, while large by the standards of TEM, only samples a miniscule part of the entire wafer and it is possible that variations in misfit and TD density occur over larger length scales.

5. Summary and conclusions

Measurements of the number of TDs and the density of misfit dislocations have been made by analysing cross-section TEM images. Although this does not give an absolute measure of

TD density ρ_{TD}, it provides valuable information about the change of ρ_{TD} through the structure. The technique was applied to five samples of GaAs:Si, each containing three $In_xGa_{1-x}As$:GaAs DFL structures of the same dimensions, but with different annealing regimes or indium content. The DFLs in all structures removed more than 90% of TDs. This led to poor counting statistics for TDs at the top of the structure even though ~1000 TDs were counted at the bottom of the structure, meaning that it was not possible to distinguish between the different structures in terms of the efficiency of the DFLs. Nevertheless some very useful information was obtained, in particular (1) in material without DFLs, the TD density decreases following a power law $\rho_{TD} = Ah^{\frac{1}{2}}$ and (2) the efficiency of DFLs at the top of the structure tends to be higher than those at the bottom. This indicates that the interaction radius, the distance below which TDs will meet and annihilate, is sensitive to ρ_{TD}.

Acknowledgments

This work was funded by the EPSRC under grant numbers EP/J013048/1 and EP/J012904/1.

References

[1] Akiyama M, Kawarada Y and Kaminishi K 1984 *J. Cryst. Growth* **68** 21–6
[2] MRS Proceedings 1991 *Symp. A—Heteroepitaxy on Silicon II* (Cambridge, MA: Materials Research Society)
[3] Grenning D A and Herzog A H 1968 *J. Appl. Phys.* **39** 2783–90
[4] Tachikawa M and Yamaguchi M 1990 *Appl. Phys. Lett.* **56** 484–6
[5] Matthews J W and Klokholm E 1972 *Mater. Res. Bull.* **7** 213–21
[6] Bolkhovityanov Y B and Pchelyakov O P 2008 *Phys.—Usp.* **51** 437–56
[7] Olsen G H *et al* 1975 *J. Appl. Phys.* **46** 1643–6
[8] Hull R *et al* 1989 *J. Appl. Phys.* **65** 4723–9
[9] Romanov A E, Fini P and Speck J S 2003 *J. Appl. Phys.* **93** 106–14
[10] Ward T *et al* 2014 *J. Appl. Phys.* **116** 063508
[11] Romanov A E *et al* 1996 *Phys. Status Solidi* b **198** 599–613
[12] Zogg H 2012 *J. Electron. Mater.* **41** 1931–5
[13] Wang G *et al* 2009 *Appl. Phys. Lett.* **94** 102115
[14] Romanov A E *et al* 1999 *J. Appl. Phys.* **85** 182–92
[15] Fertig R S III and Baker S P 2012 *Mater. Sci. Eng. a—Struct. Mater. Prop. Microstruct. Process.* **551** 67–72